

# CHRISTINE: Code for high resolution satellite mapping of optical thickness and Ångström exponent

Nicolaos I. Sifakis\*<sup>1</sup>, Christos Iossifidis<sup>2</sup> and Charis Kontoes<sup>1</sup>

<sup>1</sup>Institute for Space Applications and Remote Sensing,  
National Observatory of Athens (Metaxa and Vassileos Pavlou, GR-15236 Pendeli, Greece)

<sup>2</sup>School of Rural and Land Surveying Engineers,  
National Technical University of Athens (Heron Polytechniou 9, GR-15780 Zografou, Greece)

\*Corresponding author: email: [sifakis@space.noa.gr](mailto:sifakis@space.noa.gr);  
tel: +30-210-810.9187; fax: +30-210-613.8343

## ABSTRACT

According to the “contrast reduction” principle the aerosol optical thickness (AOT) can be retrieved and mapped over heterogeneous (such as urban) areas using a set of two satellite images of high spatial resolution: (i) one “reference image” with minimum aerosol content involving negligible AOT, and (ii) one “polluted image” with AOT to be assessed. AOT values retrieved in this way are thus relative to the reference image, and could be miscalculated when other than atmospheric changes have taken place in the time between the acquisitions of the two images. Previously developed DTA and SMA image processing codes are subject to this potential source of AOT miscalculation because the contrast reduction is applied to single spectral bands. The new CHRISTINE code takes into consideration contrast reduction in more than one spectral band and uses the Ångström’s power law to isolate atmospheric effects attributable to aerosols. Preliminary testing of the new code over the Athens urban area against results obtained using the previous codes showed a considerable improvement in terms of the area over which AOT can be retrieved with high confidence. CHRISTINE has also a complementary feature of providing information on the aerosol size distribution emerging from Ångström coefficient approximation.

**Keywords:** Satellite; remote sensing; air pollution; urban; aerosols; optical thickness; Ångström exponent.

## 1. INTRODUCTION

While satellite remote sensing is likely to become a valuable tool for assessing atmospheric pollutants at a global level<sup>[1]</sup>, applications associated to urban air quality are still infrequent. This is due, among other, to a poor collaboration between air pollution and remote sensing scientists, and to the relatively limited resources, both financially and in trained personnel, of the urban air quality monitoring sector<sup>[2]</sup>. Another important reason for this paradox is that no satellite mission aims at monitoring urban air pollution with fine spatial resolution. Few satellite sensors gather systematically data on atmospheric species, including aerosols and selected gases, such as TOMS and GOME, and more recently MOPITT, AIRS and SCIAMACHY. The spatial resolution of the previous satellite instruments is of the order of tens of kilometers which makes them relevant to global scale studies. Instruments with moderate spatial resolution (few kilometers), such as AVHRR, ATSR-2 and the geostationary GOES-8 and SEVIRI, may also provide us with information relevant to aerosols but they address large scale pollution phenomena<sup>[3][4][5][6]</sup>.

Due to the spatial scale of urban air pollution investigations the current study deals with the use of high spatial resolution (HSR) satellite sensors (with ground sampling distances from tens to a few hundreds of meters). HSR sensors, such as

TM/ETM+, HRV/HRVIR and LISS-III, while pre-dated many of the above low resolution sensors, they principally address land and sea observations rather than atmospheric investigations. Nonetheless some qualitative atmospheric observations were cited in the '70s; they concerned smoke emitted from industrial/urban sites or from forest fires<sup>[7]</sup>, assessment of pollution associated to statistical indicators<sup>[8]</sup>, and aerosol estimations over water<sup>[9]</sup>. The first quantitative pollution assessments appeared in the early '80s<sup>[10]</sup> and early attempts for pollution mapping started only in the '90s<sup>[11]</sup>. With the turn of the century the use of high resolution satellites to map the aerosol load over urban areas started progressively to receive attention from various researchers who have developed a range of techniques<sup>[12]</sup>. The passes over a given area of HSR sensors are, with respect to air pollution dynamics, infrequent, therefore satellite sensors with moderate-to-high spatial resolution (few hundreds of metres) such as MODIS and MERIS provide us, on a daily basis, with information and standardized products related to aerosol load and properties<sup>[13][14][15][16][17]</sup>. The latest generation of very high spatial resolution sensors (ground sampling distance of less than a metre), such as IKONOS-2, Quickbird, GeoEye-1 and WorldView-1, may provide ancillary information on air pollution (e.g., visible pollution plumes) or on parameters influencing pollution emissions and dispersion (e.g., land cover, traffic load, terrain roughness) as explained by Eikvil et al.<sup>[18]</sup>.

The current application deals with HSR satellite data but its findings may be extended to data with moderate-to-high resolution. HSR sensors can quantify the aerosol optical thickness (AOT) through the influence of aerosols to satellite radiometry. AOT, which is also symbolized  $\tau_a$  and is occasionally found in literature as AOD (aerosol optical depth), is a dimensionless number defined as the integral of the atmospheric extinction coefficient from the surface to the top of the atmosphere (or to the satellite). It is used to describe the amount of aerosol attenuation through scattering and absorption processes. According to Ångström<sup>[19]</sup> the spectral AOT can be described as follows:

$$\text{AOT}(\lambda) = b \lambda^{-\alpha} \quad (1)$$

where, exponent “ $\alpha$ ” is the Ångström coefficient that is inversely related to the size of scattering particles, and “ $b$ ” is referred to as the turbidity coefficient and is related to the total aerosol content. Using equation (1) allows to assess the exponential spectral variability of AOT as a function of the Ångström coefficient. The latter’s values vary between 0 and 4 depending on the size of atmospheric constituents (particles or molecules) that interfere with radiation attenuation processes. The two extreme values of the Ångström exponent, namely 0 and 4, correspond to totally reflective particles (i.e., thick clouds) and to Rayleigh type scatterers (i.e., gaseous molecules) respectively, with intermediate values corresponding to particles of different sizes and thus of variable origins. Thus the estimation of the spectral variation of AOT may directly inform on both the aerosol quantity -in terms of total column- and the size distribution of the aerosol particles. When normalised to ground level, AOT can be correlated to particle concentration (PM)<sup>[20][21]</sup>, and bridge the gap between “point measurements” derived by ground-based monitoring stations, and “spatial estimations” derived by modeling<sup>[22]</sup>.

AOT can be retrieved from HSR data using various operational methods with respective limitations. For example, the “clear water” method can be used only above water surfaces<sup>[23]</sup>, the DDV (dense dark vegetation) method requires the presence of vegetated areas<sup>[24]</sup>, and the “deep blue” method<sup>[25]</sup> has shown satisfactory results over bright targets and is applicable only to sensors with bands sensitive in the blue spectral area. The proposed CHRISTINE method is based, like the previous DTA<sup>[11]</sup> and SMA<sup>[26]</sup> methods, on the contrast reduction principle. Contrast reduction is observed in the visible and infrared spectral areas due to scattering by aerosols, and can be linked to AOT through Koschmieder’s equation<sup>[27]</sup>:

$$C/C_0 = \exp (-\text{AOT}) \quad (2)$$

where  $C$  is the observed and  $C_0$  is the real contrast of a target. From equation (2) we notice the exponential dependence of AOT on contrast reduction, which means that the latter should be particularly sensitive to assess AOT’s variations. Contrast reduction gives best results when applied over urban areas, since such areas are composed by heterogeneous and distinctly textured land parcels.

## 2. METHODOLOGY

CHRISTINE assesses, similarly to the previous DTA/SMA codes, contrast reduction on a grid superimposed to the satellite images. In the case of Landsat the grid cell comprises 17x17 pixels, a size chosen as a compromise between a grid small enough for the atmosphere to be considered homogeneous (so that AOT values are representative for any given grid cell), and large enough for the surface to be considered heterogeneous (so that contrast values are significant). While this calculation grid covers an area of 0.5 km by 0.5 km, final AOT maps correspond to the spatial resolution of the sensor, and AOT values correspond to the central pixel of the grid. The improvement that CHRISTINE brings about to AOT estimation is that contrast reduction is assessed in consecutive spectral bands while with the previous DTA/SMA codes contrast reduction was assessed in single bands. The new code uses the same basic equation (3) as DTA/SMA in order to calculate spectral AOT in each spectral band as follows:

$$\Delta\tau = \tau_2 - \tau_1 = \ln [ \sigma_1(\rho^*) / \sigma_2(\rho^*) ] \cos\theta_v \quad (3)$$

where  $\sigma_1(\rho^*)$  is the standard deviation of the reflectance values of pixels included in a grid cell on the “reference image”, and  $\sigma_2(\rho^*)$  is the standard deviation of the reflectance values of pixels included in the respective grid cell on the “examined image”,  $\Delta\tau$  is the variation of AOT from  $\tau_1$  to  $\tau_2$  (between reference and examined images), and  $\theta_v$  is the zenithal observation angle of the satellite sensor. CHRISTINE subsequently uses the spectral variation of AOT as a decision criterion in order to limit AOT retrieval over those areas where its spectral variation follows equation (1). For any two spectral bands centered at wavelengths  $\lambda_1, \lambda_2$  with respective AOT values  $\tau_{\lambda_1}$  and  $\tau_{\lambda_2}$ , it will be:

$$\text{if } \lambda_1 < \lambda_2 \text{ then it should be } \tau_{\lambda_1} > \tau_{\lambda_2} \quad (4)$$

When condition (4) is satisfied then the grid cell in which the contrast reduction is assessed is maintained for AOT retrieval otherwise the grid cell is excluded from the calculation as potentially unreliable. A tolerance of 5% on the above criterion is applied between bands 3 and 4 because AOT in the respective spectral area (i.e., red and the near infrared) is particularly low. Theoretically CHRISTINE could be applied in six of the seven Landsat TM/ETM+ spectral bands (excluding the thermal infrared band), the information, however, brought by shortwave infrared bands 5 and 7 is practically redundant. The reason is that AOT values are too low in the shortwave infrared for the atmospheric-signal-to-ground-noise ratio to be significant. Therefore only bands 1 to 4, namely in the blue, green, red and near infrared spectral areas, are retained as input to CHRISTINE. The code maintains AOT retrieved in band 2 since values in the green are higher than in longer wavelengths (i.e., red and near infrared) and not obfuscated by the molecular optical thickness in shorter wavelength (i.e., blue). Furthermore AOT in the green is sensitive to the presence of fine particles (i.e., inhalable) sized at around 2  $\mu\text{m}$ . At a final stage retrieved AOT values are classified into nine classes (including unclassified areas), where red is attributed to AOT values over 0.6. The reason for this is that it was found that AOT of about 0.6 is equivalent to the amount of pollution that can be unhealthy for sensitive groups<sup>[28]</sup>.

It should be noted that bidirectional reflectance effects are not considered in AOT calculation assuming that no significant error is induced since the code is applied only above land where, according to Tanré et al.<sup>[29]</sup>, bidirectional properties of the target are partially smoothed out by atmospheric scattering. Therefore any radiometric information associated to water bodies (mainly the sea) has to be removed. A second mask is applied to all images as buffer zone for the areas as close to the sea-land border as 17 pixels (equal to the size of one grid cell) in order to avoid contamination of AOT retrieval by sea pixels.

Along with AOT retrieval the new code addresses the type of aerosols based on an approximation of the Ångström coefficient. The Ångström exponent characterizes AOT's wavelength dependence according to equation (1), and allows approximating the aerosol size distribution. CHRISTINE uses equation (1) to calculate the Ångström coefficient at each grid cell, then applies a density slicing technique to the calculated Ångström coefficient values in order to classify aerosol sizes in four levels with each level represented by a single colour.

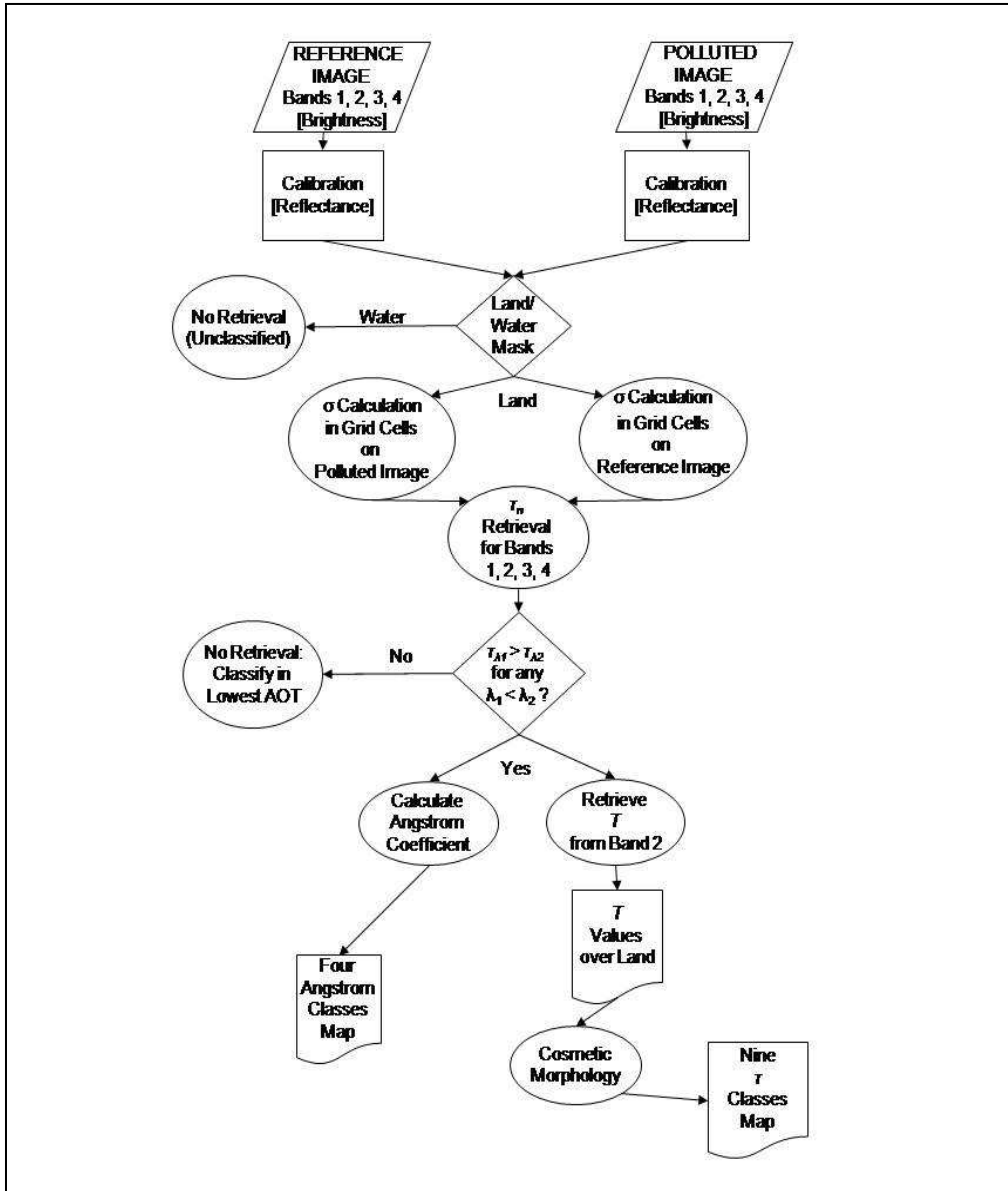


Fig. 1. Flowchart of the CHRISTINE code

The code is implemented through four main modules (Fig. 1). In each module a single executable file written in ANSI C, is invoked. The code makes use of a batch file integrating all single executable files. In all modules input files are single band 8-bit raw images, while masks are either 8-bit zeroed byte for “false” or non-zeroed bytes for “true”. The first module calibrates brightness values (digital numbers) for four spectral bands and retrieves AOT. Raw brightness values from the reference and the polluted images are input to this module. Look-up-tables (LUT) are used for the conversion of brightness values to radiance then to reflectance values in order to improve calculation time. For the same reason image buffering between RAM and disk space are extensively used. At this stage all images are multiplied by two binary

masks: (i) a pre-computed sea/land mask-image with “0” values for sea and “1” values for land, and (ii) a buffer zone to exclude retrieval over water and over areas that are closer than one grid cell to the sea-land border. Subsequently four parallel executions of equation (2) are carried out over land for bands 1, 2, 3 and 4 to retrieve AOT values. Image buffering during AOT retrieval decreases calculation execution time to one third compared to the previous DTA/SMA codes. Retrieved AOT values are input to the second module, where the code compares, at each pixel, AOT from four spectral bands according to condition (3); only the values fulfilling criterion (3) are maintained. The output of this module is composed by maintained AOT values from band 2 in a binary raw file format (single band 4-byte real floating point). In the third module CHRISTINE applies morphological “closing” as a cosmetic processing then produces a 9-class AOT map suitable for demonstration purposes. This map is in a bitmap format and produced after density slicing of retrieved AOT using a preset chromatic legend. The legend includes two classes with “unclassified” pixels: (i) masked water bodies, and (ii) areas not complying with equation (4) thus considered as non confident for AOT retrieval. Pixels of the first class are represented by black solid pixels while pixels of the second class are classified together with the lowest AOT values class (i.e., 0-0.05) thus appear as transparent. In the fourth module the average Ångstrom exponent is approximated on the basis of AOT multispectral retrieval through regression analysis on equation (1). Four Ångstrom coefficient classes are distinguished: [0, 0.5], [0.5, 1], [1, 1.5] and superior to 1.5. The final image is in a bitmap format using a 256 color pallet: 8 predefined colors, 240 grey-scaled and 8 reserved/not used.

### 3. TEST AREA AND DATA

The geographic region for testing CHRISTINE covers the Greater Athens Area (GAA). This selection was due the existence of a large body of studies and data that have already dealt with air pollution in that urban area, and to the imminent 2004 Olympic Games in Athens.



Fig. 2. 3D view of the GAA derived by a combination of a Landsat image and a digital elevation model.

Athens is a city with a history of environmental, particularly atmospheric, problems. It now accommodates a population of about 3.5 million inhabitants (census 2001). Most of the population live within the Athens basin, which is an elongated bowl oriented along a NE-SW axis with mountains on all sides (ranging from 400 to 1200 m a.m.s.l.), and the sea to the south (Saronikos Gulf) (Fig. 1). Predominant winds flow around the year in the NE-SW direction but because of the orographic setting air pollution is often confined in the basin. The climate in the GAA is typical Mediterranean with mild winters (mean seasonal air temperature of 9.9 °C), warm summers (mean seasonal air temperature of 25.8 °C) and annual rainfall of about 418 mm. Solar radiation is rather strong with average diurnal values (on a horizontal surface) of the order of 22 MJm<sup>-2</sup> in the summer and 8 MJm<sup>-2</sup> in the winter. Sea-breeze cells develop along the main NE-SW axis of the basin in late spring and the summer while during summer northerly strong (Etesian winds) usually blow. Apart from the traffic, some industrial activities exist in the western part of the GAA. Due to working hours there is, almost every day, a peak in air pollution at around 8h00 LST<sup>[30]</sup>. Since 1984 the Division of Air Quality and Noise Control (EARTH) of the Ministry of Environment, Physical Planning and Public Works is responsible for air quality monitoring in the GAA. A number of studies have been devoted to the air pollution problem in the GAA aiming at analyzing the conditions that favor air pollution episodes, via computer simulations and at experimental level<sup>[31]</sup>.

The satellite data used to test the CHRISTINE code were Landsat 5 and Landsat 7 high spatial resolution images representing the GAA. A large portion of the image data sets were acquired in the framework of the RETROPOLIS project which was concerned with a “Retrospective Mapping of Air Pollution in Athens by Satellite” for the years before 2001, when no ground measurement on aerosol concentrations (in terms of PM10) was yet available. Therefore the selection of the satellite images was based on (i) on the availability of HSR satellite data acquired before 2001 over the study area, (ii) the pollution level data from the local ground based stations. Originally only images of high quality acquired under extremely low cloud cover were considered as candidates. Secondly, as no aerosol concentration data were available before 2001, pollution levels were assessed on the basis of information on gaseous pollutants. In particular the average concentration (between all available stations) for the two basic pollutants, NO<sub>2</sub> and SO<sub>2</sub>, was calculated for each satellite acquisition date. The ratio between these spatial averages and the maximum annual value for the respective year was determined. This allowed ranking the pollution levels of each candidate satellite acquisition date according to the most polluted day of the year, then select the most polluted available for each year. Thus 100% of the selected polluted images correspond to the 20 most polluted days of the respective years, while 50% correspond to the 10 most polluted days of the respective years. This renders the selected satellite images representative in terms of pollution levels. Almost all of these images are acquired in the spring and early summer period, when the highest pollution levels in Athens are usually being recorded<sup>[32]</sup>. The selection of the so-called reference (i.e., pollution-free) images was based on the inverse procedure. From all available Landsat images acquired between 1986 and 2001 fifteen were finally selected.

#### 4. RESULTS

Processing of the selected images included a geometrical control (super-imposition) and a geo-rectification according to a topographic map. The latter was carried out using the ER Mapper 7 image processing software by applying the so-called “nearest-neighbor” algorithm in order to avoid altering the raw radiometric values and maintain the initial distribution pattern of the pixels. For the same reason no stretching or other contrast enhancement technique was applied to the histograms of the images. Subsequently all information referring to water-surface was removed by “masking” the images. The geo-rectification of the images, carried out during the preprocessing, resulted into a geometrical accuracy of the order of half a pixel.

AOT mapping was the first output of CHRISTINE. Fig. 3 depicts the results from the application of the code to twelve of the thirteen selected satellite images between 1986 and 2001. These maps depict the spatial distribution of urban aerosols over the GAA during typical pollution days. In most cases the bulk of the pollution cloud is confined inside the Athens basin around the city centre. There are also pollution spots to the west of the basin, in Thriassion, where the main industrial activity is concentrated. In many cases pollution from the centre is transported to the northern suburbs towards the foot

of Parnitha and Pendeli mountains, by the sea breeze phenomenon in the basin. Sea-breeze circulation in the GAA from the Saronikos Gulf as well as calm conditions favour the built up of air pollution episodes and, during sea breeze or weak southerly flow conditions, air pollutants may be transported from the shore inland due to the formation of the thermal internal boundary layer<sup>[33]</sup>. This is, however, the first time that this phenomenon has been observed and confirmed using high spatial resolution satellite imagery.

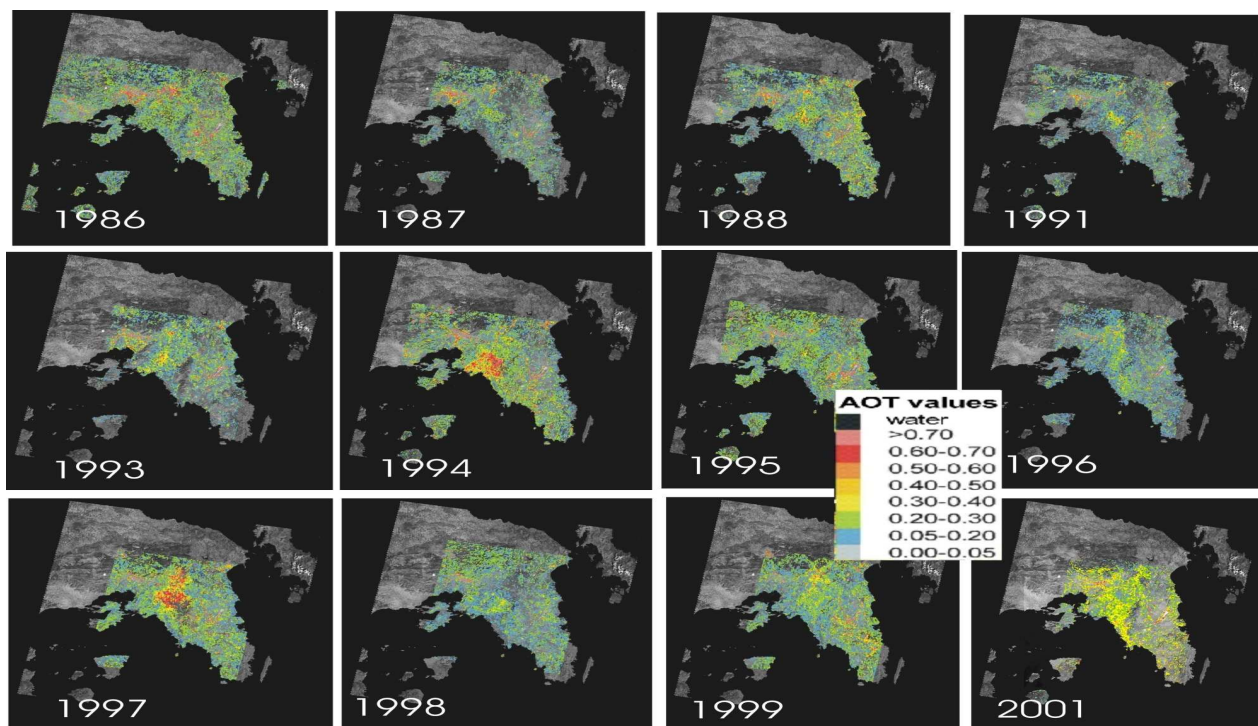


Fig. 3. AOT satellite maps over the Greatest Athens Area. Dates from top to bottom: 26.04.1994, 31.05.1995, 04.07.1996, 20.05.1997. Left column images show results obtained using SMA while right column images depict results using CHRISTINE.

The results of the new code were compared to those of the previously available SMA code. Fig. 4 juxtaposes four of the AOT maps resulted by CHRISTINE (right column) with SMA results (left column). In general when comparing the two subsets of results all maps derived by CHRISTINE contain less noise and have more clearly identified boundaries between the various AOT classes. The total area covered by unclassified AOT over land (non-confident for AOT retrieval) is always bigger in the case of the CHRISTINE implementation, since AOT is retrieved over lesser areas but with higher levels of confidence. It is significant to note that a characteristic Z-shape area with high AOT values, which is common to all SMA results, does not appear in CHRISTINE results (see Fig. 4 encircled in the first row). This Z-shaped area passing next to Mt. Ymittos and extending to the east of the mountain is, in fact, an artifact resulted by land cover changes that have occurred between the reference image and the examined images. In particular the excavations that took place around the new airport (Eleftherios Venizelos) along with part of the ring-road (Attiki Odos) in the year of 2000 (when the reference image was acquired) altered the surface in those areas resulting into an apparent contrast reduction. This was falsely interpreted by SMA as due to atmospheric aerosols resulting into high AOT values. CHRISTINE successfully managed to isolate this artifact and eliminated this area from AOT retrieval.

Some further observations that are specific to each date, and concern the performances of CHRISTINE as well as the spatial variability of air pollution in the GAA follow:

- The date of 26.04.1994 (Fig. 3 first row from top) represents a typical spring air pollution episode. High pollution levels were recorded inside the Athens basin which is clearly depicted by the AOT map. Meteorological data show an anticyclonic circulation which, combined to the transportation of warm air masses, resulted in a limited vertical development of the mixing layer. The main pollution load is accumulated over the city centre while the rest of pollution is dispersed but confined inside the Athens basin and along the south coast. When we use CHRISTINE the Z-shape artifact attributed to land cover changes is effectively masked.
- The date of 31.05.1995 (Fig. 3 second row from top) presents moderate to high pollution levels above the city centre and towards the northeastern suburbs against Ymittos Mt. Along with the Z-shape other artifacts have been masked out in the upper right part of the image (Mt. Pendeli) probably associated with wildfires distraction during the previous summer.
- The date of 04.07.1996 (Fig. 3 third row from top) is a summer image showing moderate pollution levels over the GAA. The bulk of pollution is confined in the basin mainly along a southwest-northeast axis, which is perpendicular to the coast, due to a typical sea breeze mechanism developed during springtime. In the results obtained by CHRISTINE (right image) the effect of masking of the Z-shape artifact is also pronounced in this case.
- The date of 20.05.1997 (Fig. 3 last row from top) corresponds to a second springtime pollution episode but intense pollution is more widespread around the city centre towards the north-eastern suburbs covering almost the entire Athens basin. In this case CHRISTINE has masked out all artifacts described in the previous image plus a large area on Ymittos Mt. (right in the middle of the image), which is associated with a wildfire that occurred in summer 1996.

AOT values generated by CHRISTINE are considered in relation to pollution data by comparing satellite retrieved AOT to ground based pollution. Such comparison is not always a straight forward task because satellite measurements of AOT are vertically averaged while ground based data on pollutant concentrations are point measurements. Nonetheless, since aerosol sources are on the surface, emitted particles are mainly in the troposphere and most particularly in its lowest part generally at an altitude of less than 1.5 km of altitude<sup>[33]</sup>. Hourly concentration values of pollutants recorded by the EARTH national monitoring network were used as ground truthing for AOT satellite retrieval. The EARTH network is composed by 18 stations monitoring most of the common gaseous and particulate (aerosols) air pollutant concentrations. However, PM<sub>10</sub> measurements had not been carried out by the EARTH network until 2001, thus validation is based solely on available SO<sub>2</sub> concentration measurements. Sulfur dioxide along with nitrogen dioxide while gaseous pollutants, they are the closest chemical precursors of secondary aerosols, that is, ammonium sulfates and nitrates. Fig. 5 shows a significant correlation between satellite AOT retrieval and ground based SO<sub>2</sub> in the GAA. This linear correlation of two indirect related parameters is of the order of 70%, which can be explained by the fact that ammonium sulfates are produced, in form of optically effective particles, when sulfur dioxide is oxidized into droplets of sulfuric acid, then react with ammonia in the atmosphere (part of urea synthesis)<sup>[34]</sup>. The above correlation shows that, in this case, SO<sub>2</sub> can only partly explain the aerosol spatial fluctuations since AOT depends also on other optically effective atmospheric constituents such as ammonium nitrates or soot. Using satellite images acquired after the year 2001, when PM<sub>10</sub> ground data were available, Sarigiannis et al. found a correlation of R<sup>2</sup>=0.97 between satellite based AOT and PM<sub>10</sub> in the GAA<sup>[27]</sup>.

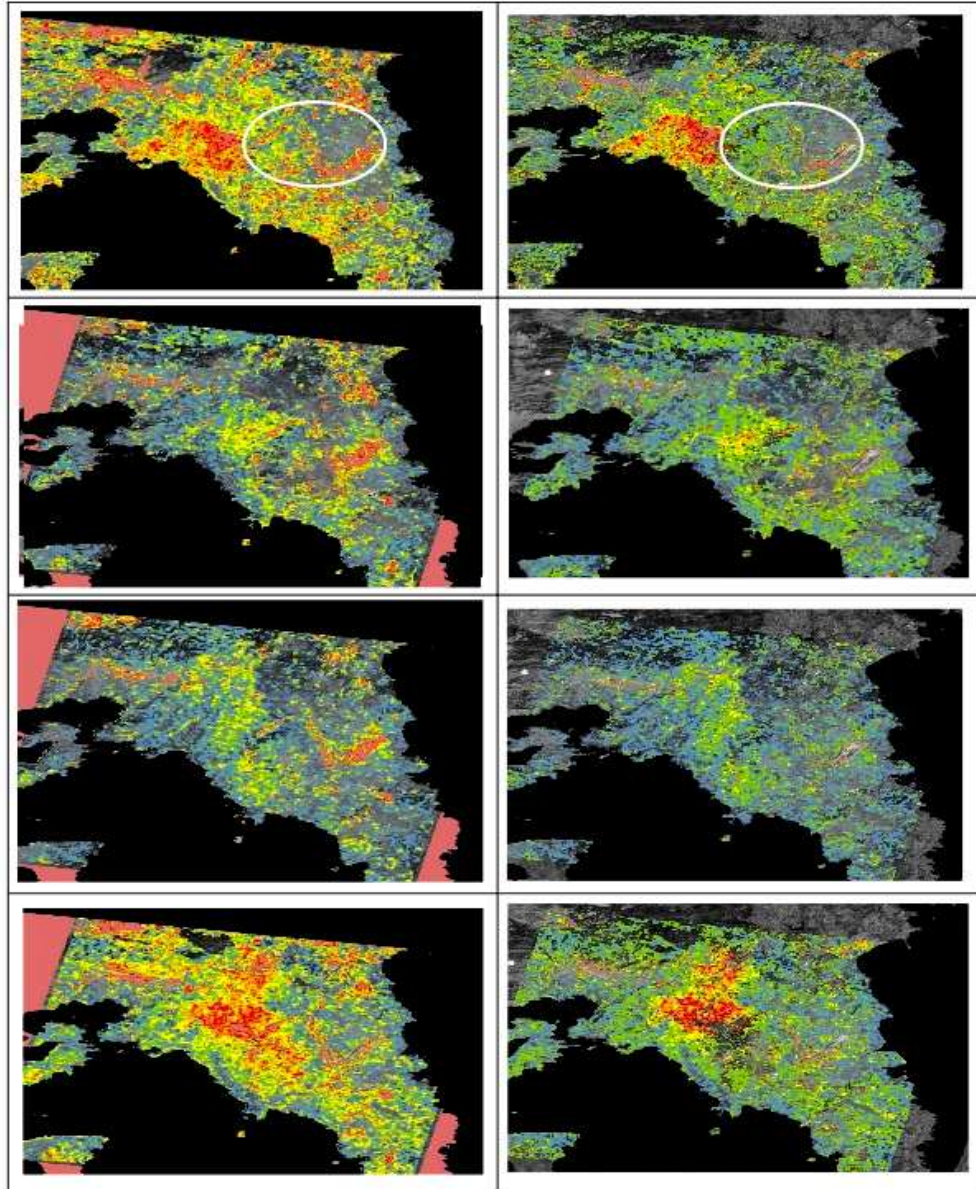


Fig. 4: AOT satellite maps over the Greatest Athens Area. Dates from top to bottom: 26.04.1994, 31.05.1995, 04.07.1996, 20.05.1997. Left column images show results obtained using SMA while right column images depict results using CHRISTINE.

The second output of CHRISTINE is the approximation of an average Ångström coefficient. While some studies have already compared experimental data and modeling estimates of AOT and Ångström coefficient over the GAA, no study to date has yet attempted to assess the Ångström coefficient on the basis of high resolution satellite data. According to Kaskaoutis et al.<sup>[35]</sup> the errors in Ångström become larger at low AOT values at least over the Athens area. Therefore the characterisation of the aerosols can best be performed under high aerosol burden conditions, as is the case for the date of 26.04.1994. Fig. 6 presents the first spatially averaged satellite map of the Ångström coefficient over the GAA derived by CHRISTINE for this date.

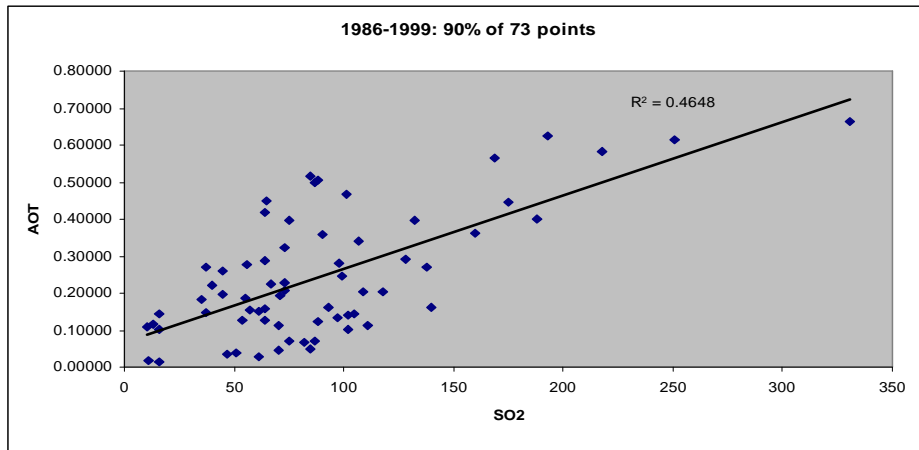


Fig.5. Satellite derived AOT vs. ground based SO<sub>2</sub> for 90% of all common available measurements.

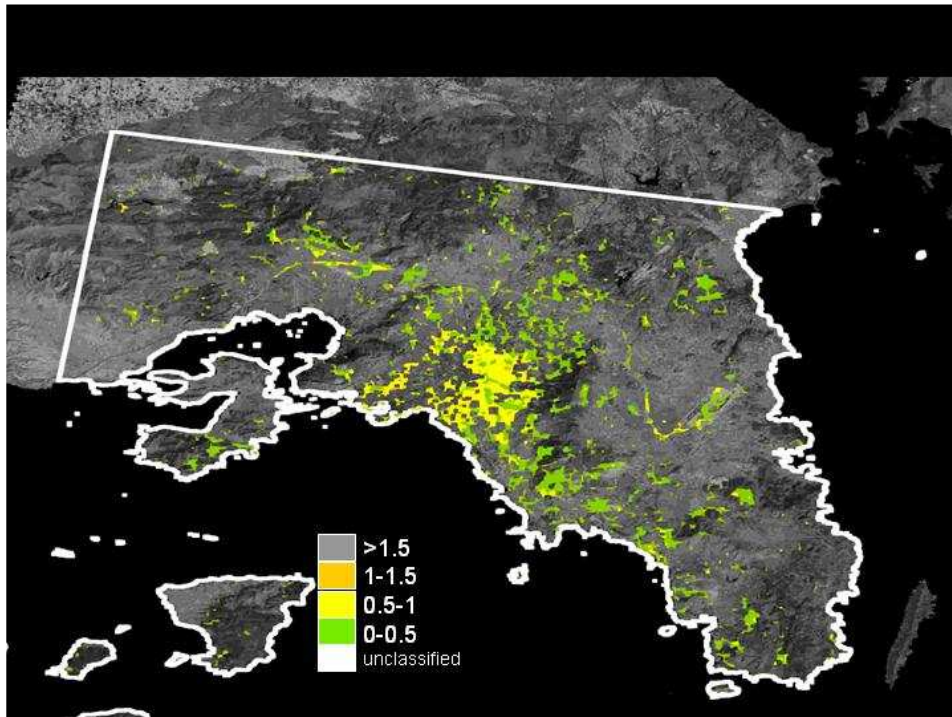


Fig. 6. Ångstrom exponent map over the GAA derived by the application of CHRISTINE to Landsat data.

Since no ground truth information with respect to particle size distribution was available our validation was based on empirical interpretations based mainly on local knowledge. First, we noticed that the Ångström exponent increases towards the city centre and western of the centre. This indicates that smaller particles predominate in these areas, which is reasonable as emission sources are located there. The Ångström exponent decreases towards the suburbs meaning that particles grow as they spread, by coagulation and humidification. In this typical pollution-episode day of the 26<sup>th</sup> of April 1994 the dominant aerosol type is characterized by an Ångström exponent varying from 1.5, close to the emission sources, to 0.5 further downstream; these figures are usual for urban hazes including dust and sea salt aerosols.

## 5. DISCUSSION

A new code and the respective CHRISTINE software code for high resolution satellite mapping of aerosol optical thickness and Ångström coefficient approximation have been developed. This code has been applied to high resolution Landsat TM/ETM+ data. The implementation has been based on the “contrast reduction” principle between a reference (with minimum aerosol content) and an examined image, as was the case with the application of the previous DTA and SMA codes. The CHRISTINE approach attempts to overcome an important limitation of the previous techniques by accommodating their sensitivity to artifacts attributed to ground reflectance variations between reference and examined image. The new code takes into consideration contrast reduction in consecutive spectral bands (i.e., in the visible and near infrared) endeavoring to decouple “atmospheric signal” from “ground noise” in AOT retrieval. In an attempt to characterise aerosol size distribution, CHRISTINE also approximates the Ångström exponent.

The new code was tested over the Greater Athens Area (GAA) in Greece well known for frequent pollution episodes. Historical Landsat 5 TM and Landsat 7 ETM+ satellite data, coinciding with characteristic pollution conditions in the period 1986 to 2001, were used for this study. Since no aerosol concentration data measurements were carried out for that period in Athens, the results from this application allowed, for the first time, the visualisation and quantification of the spatial distribution of particulate air pollution over the GAA during typical pollution situations. The comparison of AOT results obtained by the previous SMA code and CHRISTINE yielded a clear advantage of the latter technique in decoupling contrast variations attributed to the atmosphere from those attributed to ground reflectance changes associated with land cover changes between reference and examined satellite images. CHRISTINE also overcame certain speed calculation constraints, which were a limiting factor for the previous codes. A remaining limitation is that the new code, as the previous ones, it is based on the contrast reduction principle therefore its application is restricted to highly contrasted areas, favoring the application of the method over urban sites. Thus CHRISTINE is not appropriate for homogeneous areas such as extended vegetated, desert or snowed regions.

The correlation between satellite retrieved AOT values and the limited available ground based data that is, gaseous (SO<sub>2</sub>) pollutant concentration measurements, was satisfactory for this preliminary assessment. CHRISTINE also returned a rough approximation of the dominant aerosol size distribution categories on the basis of Ångström exponent calculation. Future work will address an extended validation of these results over other urban sites.

Using Landsat TM/ETM+ data allowed for the production of AOT maps with ground sampling distance of 30 metres. Information on the distribution of aerosols was extremely dense in comparison to ground based monitoring networks. This kind of spatial information is particularly useful over complex urban terrains with street canyons, building blocks and topography that continuously modulate the diffuse and advective transport of pollutants. The infrequent overpasses of high spatial resolution satellites are, nonetheless, an obvious drawback to the monitoring of dynamic phenomena such as air pollution. The use of satellite data acquired by sensors with daily overpasses, such as MODIS or MERIS, would enable aerosol optical thickness retrieval on a daily basis for the assessment of short-term exposure to pollutants. However these data have much coarser resolution, which is less appropriate for investigations in urban sites. High resolution satellite data may be used to improve air quality monitoring in urban areas mainly by supplementing the spatial nature of the existing urban monitoring networks. Detailed space resolved estimates on air pollution over urban

areas by satellite can thus be useful towards complying with the European air quality Framework Directive 96/62/EC, and also lead to improvements in air quality monitoring networks deployment.

## 6. REFERENCES

- [1] King, M. and Greenstone, R., 1999. EOS Reference Handbook: A Guide to NASA's Earth Science Enterprise and the Earth Observation System. NASA/GSFC, Greenbelt.
- [2] Engel-Cox, J., Hoff, R.M and Haymet, A.D.J., 2004. Recommendations on the use of satellite remote-sensing data for urban air quality. *Journal of the Air & Waste Management Association* 54 (11), 1360-1371.
- [3] Kaufman, Y.J., Fraser, R.S. and Ferrare, R.A., 1990. Satellite Remote Sensing of large scale air pollution: Method. *J. of Geophysical Research*, 95, 9895-9909.
- [4] Holben, B., Vermote, E., Kaufman, Y.J., Tanré, D. and Kalb, V., 1992. Aerosol Retrieval Overland from AVHRR Data – Application for Atmospheric Correction. *IEEE Transaction on Geoscience and Remote Sensing*, 30, 212-222.
- [5] Costa, M.J., Cervino, M., Cattani, E., Torricella, F., Levizzani, V., Silva, A.M. and Melani, S., 2002. Aerosol characterization and optical thickness retrievals using GOME and METEOSAT satellite data. *Meteorology and Atmospheric Physics*, 81, 289-298.
- [6] Popp, C., Hauser, A., Foppa, N. and Wunderle S., 2007. Remote sensing of aerosol optical depth over central Europe from MSG-SEVIRI data and accuracy assessment with ground-based AERONET measurements. *J. Geophys. Res.*, 112, D24S11.
- [7] Short, N.M., Lowman Jr., P.D., Freden, S.C. and Finch Jr., W.A., 1976. Mission to Earth: Landsat Views of the World. NASA, Scientific and Technical Information Office, Washington D.C., 459 p.
- [8] Potter, J.F. and Medlowitz, M.A., 1975. On the determination of Haze Levels from Landsat Data. *Proc. of the 10<sup>th</sup> Int. Symposium on Remote Sensing of the Environment*, Ann Arbor, 695-703.
- [9] Griggs, M., 1975. Measurement of atmospheric optical thickness over water using ERTS-1 data. *J. Air Poll. & Control Ass.*, 25, 622-626.
- [10] Fraser, R.S., Kaufman, Y.J. and Mahoney, R.L., 1984. Satellite Measurements of Aerosol Mass and Transport. *Atm. Environment*, 18, 2577-2584.
- [11] Sifakis, N. and Deschamps, P.Y., 1992. Mapping of Air Pollution Using Spot Satellite Data. *Photogrammetric Engineering and Remote Sensing*, 58, 1433-1437.
- [12] Kocifaj, M. and Horvath, H., 2005. Retrieval of size distribution for urban aerosols using multispectral optical data. *Journal of Physics: Conference Series* 6, 97–102.
- [13] Chu, D.A., Kaufman, Y.J., Zibordi, G., Chern, J.D., Jietai, M. Chengcai, L. and Holben, B.N., 2003. Global monitoring of air pollution over land from the Earth Observing System-Terra Moderate Resolution Imaging Spectroradiometer (MODIS). *Journal Of Geophysical Research*, 108, 4661.
- [14] Von Hoyningen-Huene, W., Freitag, M. and Burrows, J.B., 2003. Retrieval of aerosol optical thickness over land surfaces from top-of-atmosphere radiance. *J. Geophys. Res.*, 108(D9), 4260.
- [15] Tang, J., Xue, Y., Yu, T. and Guan, Y.N., 2005. Aerosol optical thickness determination by exploiting the synergy of TERRA and AQUA MODIS. *Remote Sensing of Environment*, 94, 327-334.
- [16] Liang, S., Zhong, B. and Fang, H., 2006. Improved estimation of aerosol optical depth from MODIS imagery over land surfaces. *Remote Sensing of Environment*, vol. 104, no. 4, 416-425.
- [17] Kokhanovsky, A.A., Breon, F.M., Cacciari, A., Carboni, E., Diner, D., Di Nicolantonio, W., Grainger, R.G., Grey, W.M.F, Höller, R., Lee, K.H., Li, Z., North, P.R.J., Sayer, A.M., Thomas, G.E. and von Hoyningen-Huene, W., 2007. Aerosol remote sensing over land: A comparison of satellite retrievals using different algorithms and instruments. *Atmospheric Research*, 85, 372-394.
- [18] Eikvil, L., Aurdal, L. and Koren, H., 2009. Classification-based vehicle detection in high-resolution satellite images. *ISPRS Journal of Photogrammetry and Remote Sensing*, 64, 65-72.
- [19] Ångström, A., 1961. Technique of determining turbidity of the atmosphere. *Tellus*, 13, 214.
- [20] Jiang, X., Liu, Y. and Ming Jiang, B.W., 2007. Comparison of MISR aerosol optical thickness with AERONET measurements in Beijing metropolitan area. *Remote Sensing of Environment*, 107, 45-53.

- [21] Liu, Y., Franklin, M., Kahn, R. and Koutrakis, P., 2007. Using aerosol optical thickness to predict ground-level PM<sub>2.5</sub> concentrations in the St. Louis area: A comparison between MISR and MODIS. *Remote sensing of Environment*, 107, 33-44.
- [22] Sarigiannis, D., Soulakellis, N. and Sifakis, N., 2004. Information Fusion for Computational Assessment of Air Quality and Health Effects. *Photogrammetric Engineering and Remote Sensing*, 70, 235-245.
- [23] Gordon, H.R. and Clark, D.K., 1981. Clear water radiances for atmospheric correction of Measurements of atmospheric optical thickness over water using ERTS-1 data. *Journal of Air Pollution Control Association*, 25, 622-626)
- [24] Kaufman, Y.J. and Sendra, C., 1988. Algorithm for atmospheric corrections. *International Journal of Remote Sensing*, 9, 1357-1381.
- [25] Hsu N.C., Tsay S.C., King M.D. and Herman J.R., 2004. Aerosol Properties Over Bright-Reflecting Source Regions. *IEEE Trans. Geosci. Remote Sens.*, 42 (3), 557-569.
- [26] Sifakis, N., Soulakellis, N. and Paronis, D., 1998. Quantitative Mapping of Air Pollution Density Using Earth Observations: A New Processing Method and Application to an Urban Area. *International Journal of Remote Sensing*, 19, 3289-3300.
- [27] Middleton, W.E.K., 1952. *Vision Through the Atmosphere*. University of Toronto Press.
- [28] Szykman, J., White, J., Pierce, B., Al-Saadi, J., Neil, D., Kittaka, C., Chu, A., Remer, L., Gumley, L. and Prins, E., 2004. Utilizing MODIS satellite observations in near-realtime to improve AIRNOW next day forecast of fine particulate matter. In: *Sixth Conference on Atmospheric Chemistry, PM2.5*. Paper 1.2. American Meteorological Society, Seattle, WA.
- [29] Tanre, D., Herman, M., Deschamps, P.Y. and Lefte, A., 1997. Atmospheric modeling for space measurements of ground reflectances including bi-directional properties. *Applied Optics*, 18, 3587-3594.
- [30] Kambezidis, HD., Tulleken, R., Amanatidis, G.T., Paliatsos, A.G. and Asimakopoulos, D.N., 1995. Statistical evaluation of selected air pollutants in Athens, Greece. *Environmetrics*, 6, 349-361.
- [31] Scheff, P.A. and Valiozis, C., 1990. Characterization and source identification of respirable particulate matter in Athens, Greece. *Atmos. Environ.*, 24A, 203-211.
- [32] Lalas, D.P., Asimakopoulos, D.N., Deligiorgi, D.G. and Helmis C., 1983. Sea-breeze circulation and photochemical pollution in Athens. *Atmos. Environ.*, 17, 1621-1632.
- [33] Lenoble, J., 1993. *Atmospheric radiative transfer*. Deepak Publishing, Hampton, VA.
- [34] Colls, J., 1997. *Air Pollution: An introduction*. E & FN Spon (publisher), London, 341 p.
- [35] Kaskaoutis, D.G., Kambezidis H.D., Adamopoulos A.D. and Kassomenos, P.A., 2006. Comparison between experimental data and modeling estimates of aerosol optical depth over Athens, Greece. *Journal of Atmospheric and Solar-Terrestrial Physics*, 68, 1167-1178.